

# Effect of calcium and potassium on $V_2O_5/ZrO_2$ catalyst for oxidative dehydrogenation of propane: a comparative study

Mahuya De and Deepak Kunzru\*

Department of Chemical Engineering, Indian Institute of Technology, Kanpur, 208016, India

Received 11 January 2005; accepted 12 April 2005

The effect of calcium and potassium on the physiochemical properties and performance of  $V_2O_5/ZrO_2$  catalyst for oxidative dehydrogenation of propane was studied in the temperature range of 385–400 °C. The vanadia loading was kept constant at 5  $VO_x/nm^2$  and the atomic ratio A/V (A = Ca, K) was varied from 0.05 to 0.75. The vanadia surface structure was investigated using X-ray diffraction analysis (XRD), electron paramagnetic resonance (EPR), Raman spectroscopy and X-ray photoelectron spectroscopy (XPS). The redox property of the catalysts was studied by temperature programmed reduction (TPR) and temperature programmed oxidation (TPO) whereas surface acidity was measured by temperature programmed desorption (TPD) of ammonia. Calcium and potassium both interact with the surface V=O and stabilize the +5 oxidation state of vanadium. Interaction between calcium and vanadium was more intense though surface concentration of calcium was lower than that of potassium. For doped catalysts, the activity was lower due to an increase in reduction temperature as well as a lower extent of reduction and increased resistance to undergo redox cycles. On the other hand, removal of surface acidic sites by the dopants increased the propene selectivity. Potassium was more effective in decreasing the activity and increasing the propene selectivity.

**KEY WORDS:** Vanadia–zirconia; calcium; potassium; oxidative dehydrogenation; propane; temperature-programmed reduction; temperature-programmed desorption.

## 1. Introduction

Supported vanadia catalysts have been extensively used for study of oxidative dehydrogenation (ODH) of hydrocarbons. The most commonly used supports are silica, alumina and titania. Recently zirconia has been used, either as a single or mixed oxide support. The characteristics that favor zirconia over the conventional supports include, strong interaction with the active metal phase resulting in higher dispersion, higher thermal and chemical stability and unique combination of acid- base and reducing -oxidizing properties.

The activity and selectivity of supported vanadia catalysts are strongly affected by the oxidation state and molecular structure of surface vanadia species, which in turn depend upon the nature of support, preparation methods and amount of vanadia content. The other important factor that strongly affects the physicochemical properties of the catalyst is the presence of additives.

Limited literature is available on the effect of additives on the  $V_2O_5/ZrO_2$  system. Albrecht *et al.* [1] studied the alkali modified  $V_2O_5/ZrO_2$  catalyst for ODH of propane. They observed that all the alkali metals (Li, Na and K) lowered the activity of the catalyst. Sodium modified  $V_2O_5/ZrO_2$  was tested for propan-2-ol reaction by Toda *et al.* [2]. The decrease in propene formation was attributed to the decrease in both Bronsted and

Lewis acid sites due to sodium addition. Feng *et al.* [3] reported that calcium doped zirconia improved the selectivity of formation of isobutane and isobutene from synthesis gas. They attributed this increase to the increased basic character of calcium modified zirconia. Ohno *et al.* [4] studied the effect of addition of calcium to  $V_2O_5/ZrO_2$  for reduction of NO by propane.

The present study investigates and compares the effect of addition of calcium and potassium on the physiochemical properties of  $V_2O_5/ZrO_2$  catalyst. The A/V (A = Ca, K) atomic ratio was varied to investigate the effect of loading on the redox property and acidity of the catalyst. The consequent effect on the performance of the catalyst for oxidative dehydrogenation of propane was also studied. The redox property of the catalyst was characterized by temperature programmed reduction (TPR) and temperature programmed oxidation (TPO), whereas temperature programmed desorption (TPD) of  $NH_3$  were used to determine acidic sites of the catalyst. To further elucidate the surface vanadia structure, the catalysts were characterized by Raman Spectroscopy, XPS, EPR, X-ray diffraction and surface area measurements.

## 2. Experimental

### 2.1. Catalyst Preparation

The  $V_2O_5/ZrO_2$  catalysts were prepared by wet impregnation method.  $ZrO_2$  was impregnated by a solution containing  $NH_4VO_3$  and  $C_2H_2O_4$  in 1:2 molar

\*To whom correspondence should be addressed.

E-mail: dkunzru@iitk.ac.in

ratio and calcined at 600 °C. For the modified catalyst,  $Ca(NO_3)_2$  and  $KNO_3$  were added to the impregnating solution in the required amounts. The A/V ratio was varied from 0.05 to 0.5. For all the catalysts, the vanadium loading was kept constant at 6.3 wt%, corresponding to a vanadia surface density of 5  $VO_x/nm^2$ . This surface density was chosen as it gave the highest activity and selectivity for ODH of propane on undoped  $V_2O_5/ZrO_2$  catalyst [5]. The undoped catalyst has been designated as 5V whereas the doped catalysts have been designated as  $A_xV$  ( $A=Ca, K$ ), where x represents the A/V atomic ratio.

## 2.2. Catalyst Characterization

The surface area of a catalyst sample was measured by nitrogen physisorption using the dynamic pulsing technique on a Micromeritics Pulse Chemisorb 2705 unit. The total gas flow rate (30%  $N_2$  in He) was maintained at 16 cc/min. Prior to surface area determination, the sample was pretreated in a flow of helium (20 cc/min) at 30 °C for 45 min. X-ray diffraction spectra were obtained on a Reich Seifert (Germany) Iso Debye Flex X-ray diffractometer using Ni filtered monochromatic  $Cu K\alpha$  radiation of wavelength 1.5418 Å. Scans were made in the  $2\theta$  range of 15°–80° at a scanning rate of 0.3 and 3.0°/min. Raman spectra at dehydrated conditions were recorded with Renishaw System 1000. Ar laser (514 nm, 25 mW, Spectra Physics) source was used. The power on the sample was 4 mW and acquisition time was 300 s. The EPR spectra were recorded using a Bruker – ER041X Microwave Bridge X-Band at 120 K and 298 K. A microwave frequency of 9.44 GHz with 2G modulation amplitude and 100 KHz modulation frequency was used. ESCA – 3000 electron spectrometer from V.G.Microtech was used to record the XPS spectra. The monochromatic  $Al K\alpha$  (1486.6 eV) was used as the excitation source. The high resolution XPS spectra were acquired at room temperature and high vacuum ( $1 \times 10^{-10}$  torr). The binding energy scale was referenced against  $C1s = 285$  eV line.

Temperature programmed reduction (TPR), temperature programmed oxidation (TPO) and temperature programmed desorption (TPD) studies were performed on the Micromeritics Pulse Chemisorb 2705. For each test, 50 mg of sample was pretreated in an oxidative atmosphere (5%  $O_2$  in He) at 500 °C for 30 min and cooled to 250 °C in the same mixture. The sample was then purged with helium and cooled to room temperature. For TPR studies, preoxidized samples were reduced in a flow of 5%  $H_2$  in argon. For TPO, 5%  $O_2$  in He was used as the carrier gas. Each TPR cycle was followed by a TPO cycle. For each TPR/TPO test, the carrier gas flow was maintained at 30 ml/min with a heating rate of 10 K/min. For  $NH_3$  - TPD the preoxidized samples were saturated with pulses of  $NH_3$  vapor at 120 °C followed by flushing in helium at 150 °C for

2 h. Temperature programmed desorption was carried out in flowing helium (30 ml/min) from 150 °C to 550 °C at rate of 20 K/min.

## 2.3. Catalyst Activity Measurements

The activity of the catalysts for ODH of propane was measured in the temperature range of 385–450 °C at atmospheric pressure using a tubular downflow quartz reactor. The feed mixture contained propane, oxygen and nitrogen in the molar ratio of 4/4/92. The mass of the catalyst was varied from 10 to 50 mg and the total flow rate from 50 to 150 cc/min. Prior to testing, the catalyst was treated in a flow of oxygen at 500°C for 30 min. The average run length was 30 min. The reaction products were analyzed online by two gas chromatographs. For all the runs reported, the carbon balance was  $100 \pm 5$  %. At the highest reaction temperature used in this study, the catalysts showed no significant deactivation.

Catalytic activities have been expressed in terms of conversion of propane (%) and selectivity (%), defined as:

$$\text{Conversion(\%)} = \frac{\text{moles of carbon in products}}{\text{total moles of carbon in exit gas}} \times 100$$

$$\text{Selectivity of product 'X' (\%)} = \frac{\text{moles of carbon in product 'X'}}{\text{total moles of carbon in products}} \times 100$$

## 3. Results

### 3.1. Characterization study

The surface area of the catalysts decreased with increasing amount of dopants. No significant difference was observed for calcium and potassium (Table 1). The X-ray diffraction spectra of undoped and doped  $V_2O_5/ZrO_2$  catalysts are shown in figure 1. In the undoped catalyst, the tetragonal phase was the major one, characterized by the peak at  $2\theta = 30.4^\circ$ . The monoclinic phase was characterized by peaks at  $2\theta = 28.5^\circ$  and  $31.6^\circ$  [6,7]. Though the peak at 28.5 was prominent but the

Table 1  
Variation of surface area with A/V ratio ( $A=Ca, K$ )

Catalyst	Surface area ( $m^2/g$ )
5V	82.9
$Ca_{0.05}V$	81.6
$Ca_{0.1}V$	75.7
$Ca_{0.5}V$	69.3
$K_{0.05}V$	80.5
$K_{0.1}V$	78.9
$K_{0.5}V$	75.7

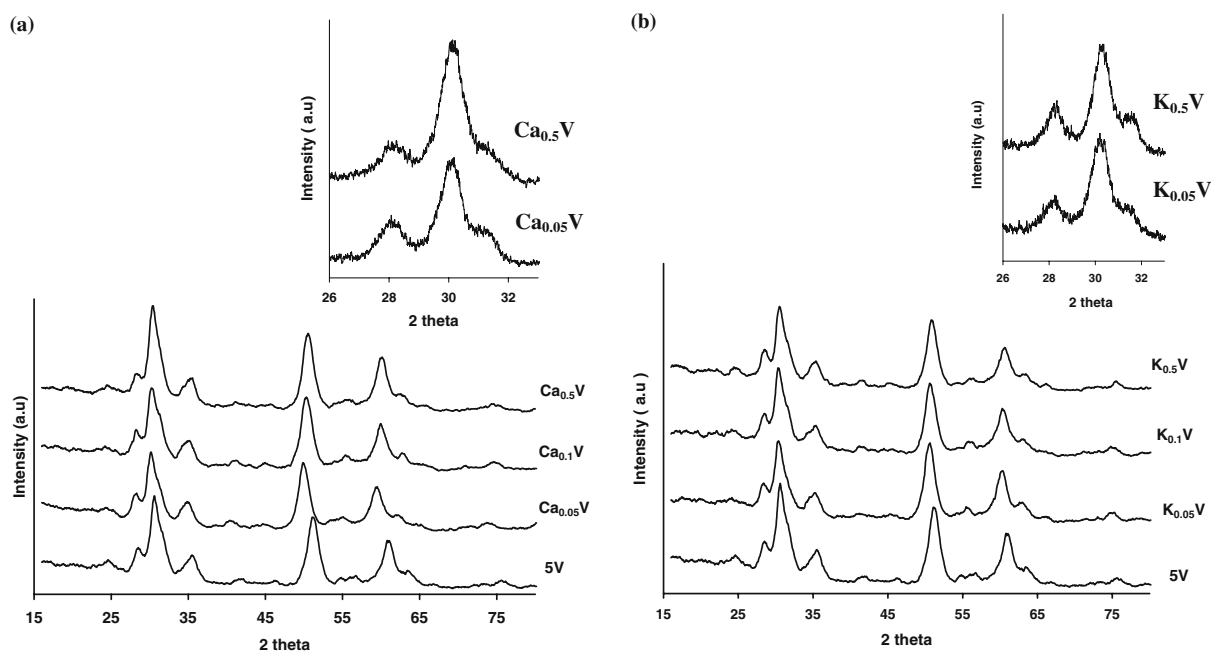


Figure 1. XRD pattern of undoped and doped  $V_2O_5/ZrO_2$  catalyst (a)  $Ca_xV$  (b)  $K_xV$ .

peak at  $31.6^\circ$  appeared only as a shoulder to the tetragonal peak. No peak due to crystalline vanadia ( $2\theta = 20.3^\circ$  and  $26.2^\circ$ ) was observed in the undoped catalyst. At low loadings ( $A/V < 0.1$ ), the dopants had no significant effect on the phase structure; however at high loading ( $A/V = 0.5$ ) both calcium and potassium modified the phase distribution. The blowup of Figure 1 in the range  $2\theta = 26^\circ$  to  $32^\circ$  shows that on increasing the loading from  $A/V = 0.05$  to  $0.5$ , for calcium, the intensity of the monoclinic peaks decreased while for potassium at high loading ( $K/V = 0.5$ ) an increase was observed. However, no new crystalline or mixed phase was observed in any of the catalysts. Absence of peaks of crystalline vanadia shows that the vanadium was well dispersed in all the catalysts and addition of dopants had no significant effect on the dispersion.

The dehydrated Raman spectra of the undoped and doped catalysts are shown in figure 2. The prominent peaks at 268, 325, 382, 474, 615 and  $640\text{ cm}^{-1}$  in the spectra of undoped catalyst can be ascribed to the tetragonal  $ZrO_2$  phase [8] and the broad band from 700 to  $970\text{ cm}^{-1}$  is characteristic of V–O–V stretching mode of polyvanadate species [9,10]. Wachs *et al.* [11] assigned the  $1034\text{ cm}^{-1}$  peak to the terminal V=O in dehydrated surface polyvanadate species and the band at  $1020\text{ cm}^{-1}$  to terminal isolated surface vanadate species. In this study, a peak with maxima around  $1030\text{ cm}^{-1}$  was observed and can be assigned to the stretching of the terminal V=O bond in vanadyl species, but cannot be exclusively assigned to either polyvanadate or isolated V=O. This peak shifted to lower temperature with addition of potassium but disappeared on Ca doping. Some of the zirconia peaks were also blurred in the

doped catalyst. Compared to the undoped catalyst, there was a significant increase in the intensity of the band at  $268\text{ cm}^{-1}$  in the calcium doped catalyst ( $Ca/V = 0.5$ ). Platero *et al.* [8] have associated the increase in the intensity of this band to the tetragonal modification of zirconia due to calcium as was also observed in XRD results. The  $268\text{ cm}^{-1}$  peak was not affected in the presence of potassium. The broad band at  $700\text{--}1000\text{ cm}^{-1}$  corresponding to polyvanadate was also modified in presence of dopants.

The XPS analysis showed that in both fresh undoped and doped  $V_2O_5/ZrO_2$  catalysts, most of the vanadium was present in +5 oxidation state [ $V\ 2p_{3/2} = 517.5 \pm 0.1\text{ eV}$ ] and zirconia in +4 state ( $3d_{5/2} = 182.3 \pm 0.2\text{ eV}$ ). Surface calcium was not observed at lower loading ( $\leq Ca/V = 0.1$ ). At higher loading ( $Ca/V = 0.75$ ), a small peak was observed at  $350.2\text{ eV}$  corresponding to  $Ca\ 2p_{1/2}$ . The  $Ca\ 2p_{3/2}$  peak was not observed as it merged with  $Zr\ 3p$  peak. For potassium doped catalysts, surface potassium ( $K\ 2p_{3/2} = 293.4\text{ eV}$ ) was observed at all loadings. Intensity of the peak increased with increase in  $K/V$  ratio. Table 2 compares the surface and bulk vanadium concentration of the catalyst. The higher value of surface concentration compared to bulk implies that most of the vanadium is retained on the surface.

Figure 3a shows the EPR spectra of fresh doped and undoped  $V_2O_5/ZrO_2$  catalysts at 120 K. The weak signals can be assigned to the  $V^{+4}$  in an axially symmetric environment. The hyperfine structure arise due the interaction between the unpaired electron  $3d^1$  with the nuclear magnetic moment vanadium ( $I = 7/2$ ). The  $g$  values and the hyperfine coupling constants of the  $V^{+4}$

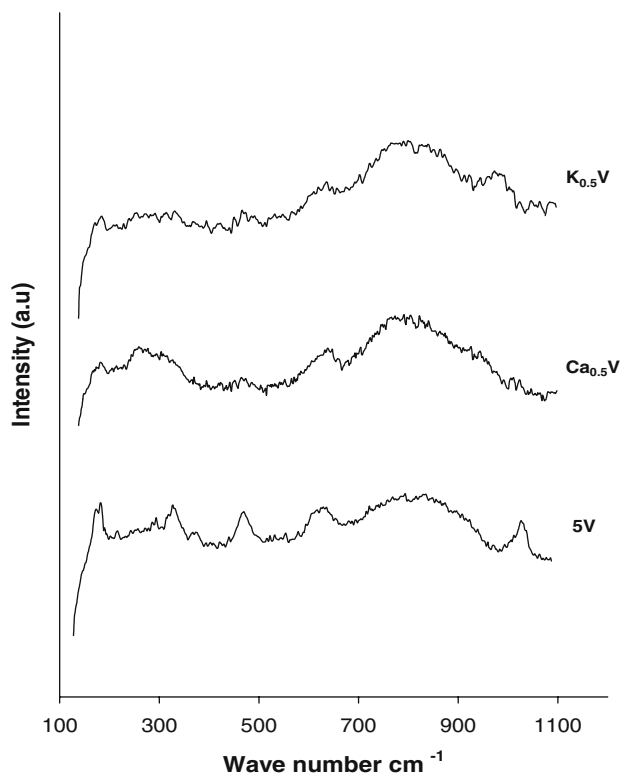


Figure 2. Dehydrated Raman spectra of calcium and potassium doped  $V_2O_5/ZrO_2$  catalyst.

signal were  $g_{||} = 1.98$ ,  $g_{\perp} = 2.03$ ,  $A_{||} = 174$  G, and  $A_{\perp} = 66$  G. Similar spectra were also observed at room temperature but the intensity was lower. The EPR signal detected at room temperature is assigned to the octahedral  $V^{+4}$  since it is reported that detection of tetrahedral  $V^{+4}$  is possible only at low temperature due to relaxation effects [12]. The additional detection of tetrahedral species might be the reason for an increase in the intensity at low temperature. The detection of signal both at room temperature and 120 K suggests the presence of both tetrahedral and octahedral  $V^{+4}$  species on the surface. However, more detailed study is required to establish the coordination environment of the  $V^{+4}$  species in these catalysts. The spectra of used catalysts (figure 3b) recorded an increase in the intensity of  $V^{+4}$  signal. This indicates that surface vanadia was reduced under oxidative dehydrogenation reaction conditions. Previous studies have also shown an increase in

concentration of reduced centers on catalyst surface after ODH reactions [13]. The increase in the intensity was less for doped catalysts. In both fresh and used conditions, intensity was lowest for calcium doped catalyst. Therefore, it can be concluded that both calcium and potassium stabilize the +5 oxidation state of vanadium and the effect is more for calcium. The stabilization of +5 state of vanadium by potassium for  $V_2O_5/Al_2O_3$  has also been reported earlier [14].

The TPR profiles of the catalysts are shown in figure 4. The undoped and doped  $V_2O_5/ZrO_2$  catalysts ( $\leq A/V = 0.5$ ) reduced at lower temperature compared to bulk vanadia [5], signifying strong metal-support interaction. The TPR profile for undoped catalyst consisted of a main reduction peak centered at 439 °C with a shoulder at 414 °C. The extent of reduction, defined as the ratio of the actual hydrogen consumed to the theoretical hydrogen consumed per gm of catalyst (assuming complete reduction from  $V^{+5}$  to  $V^{+3}$ ), was found to be 0.81 for the undoped catalyst (table 3). The original TPR profiles were deconvoluted into Gaussian peaks and the fit corresponding to minimum error was taken as the best fit. The reduction temperatures and areas under the deconvoluted peaks for all the catalysts are also given in Table 3. The area ratio of the two peaks, ( $P_2/P_1$ ) and reduction temperatures depend on the nature and A/V ratio. Upto a loading of  $Ca/V = 0.1$ , calcium did not significantly affect the TPR profile of  $V_2O_5/ZrO_2$  but the extent of reduction decreased. For potassium, an increase in the reduction temperature was observed for  $K_{0.1}V$  catalyst. At high loading,  $A/V = 0.5$ , there was a significant increase in reduction temperatures as well as in  $P_2/P_1$  ratio with simultaneous decrease in the extent of reduction.

To check the effect of dopants on the activity and stability of the  $V_2O_5/ZrO_2$  catalyst, successive TPR cycles were carried out. When the samples were heated from room temperature to 600 °C, no change was observed in the reduction profile for the undoped catalyst. For doped catalysts at high loading,  $A/V = 0.5$ , the reduction peak shifted by 7–10 °C to higher temperature. In the next set of experiments, the sample was heated upto 800 °C in the first TPR cycle. This resulted in shifting of the reduction peak of the undoped catalyst to higher temperature (519 °C) but without any significant change in the nature of the profile. In contrast, for doped catalysts multiple peaks appeared in the TPR profiles (not shown), with reduction peaks shifting to still higher temperatures, showing that vanadia surface structure was affected.

Temperature programmed desorption of ammonia was used for determination of surface acidity of the catalysts. The desorption profiles of the catalysts are shown in figure 5. The profiles were deconvoluted into two peaks corresponding to the best fit [15,16]. Total amount of  $NH_3$  desorbed by the different catalysts and desorption temperatures are presented in table 4. For

Table 2  
Surface and bulk concentration of vanadium in undoped and doped  $V_2O_5/ZrO_2$

Catalyst	V / V + Zr (bulk)	V / V + Zr (XPS)	A/V (A = K, Ca)
5V	0.16	0.37	0.0
$Ca_{0.1}V$	0.16	0.31	—
$Ca_{0.75}V$	0.16	0.34	low
$K_{0.1}V$	0.16	0.39	0.20
$K_{0.5}V$	0.16	0.41	0.46

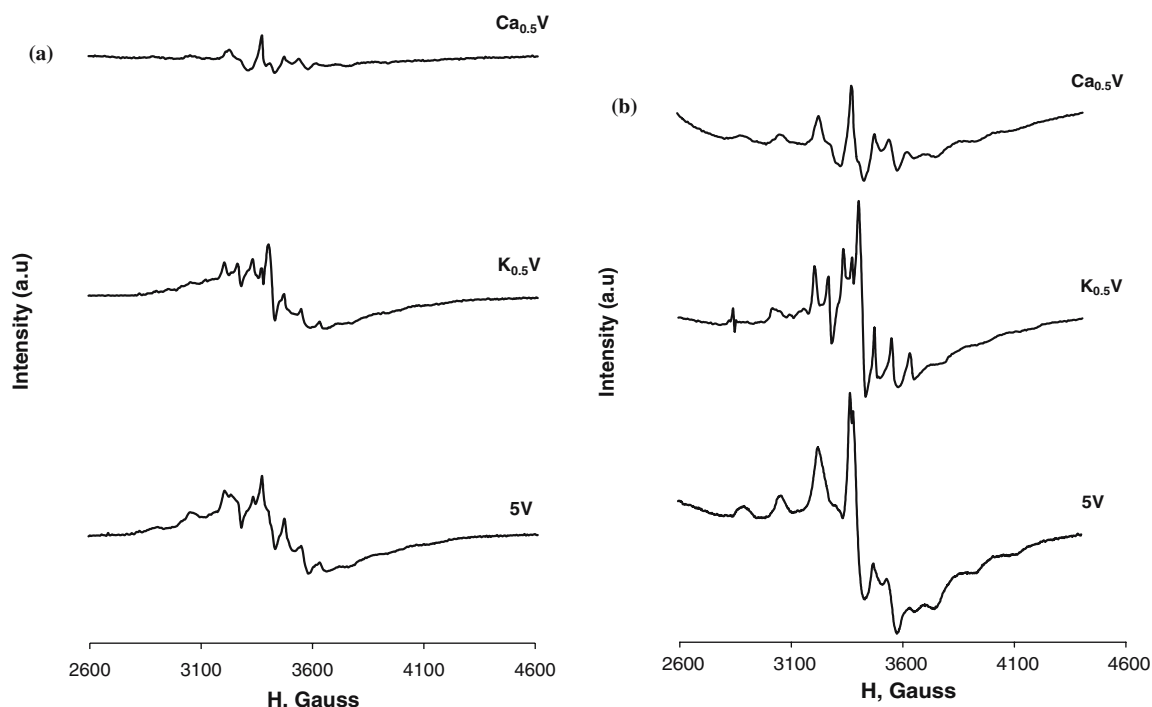


Figure 3. EPR spectra of undoped and doped  $V_2O_5/ZrO_2$  catalyst (a) fresh catalyst (b) used catalyst.

undoped  $V_2O_5 / ZrO_2$ , the low temperature peak was centered around 265 °C whereas the other peak around 322 °C. Since the strength of acid sites is related to the desorption temperature, higher desorption temperature correspond to greater strength of the acid sites. The undoped catalyst was mostly acidic in nature as shown by high ammonia uptake and higher concentration of stronger acid sites. Addition of calcium or potassium lowered the total amount of desorbed  $NH_3$  implying decrease in total acid strength. At the same loading, potassium doped catalyst was less acidic. Addition of potassium had no major effect on the distribution of acid sites or the desorption temperature, whereas, addition of calcium decreased the concentration of stronger acid sites with simultaneous increase in the weaker sites. At high calcium loading, the strong acid sites were reduced by more than half. However, calcium shifted the peaks to higher temperature implying increase in strength of the acidic sites. Adsorption of ammonia was very low for  $K_{0.5}V$  catalyst and the desorption profile is not shown.

### 3.2. Catalyst Activity

The activities of the undoped and doped  $V_2O_5/ZrO_2$  catalysts were compared at identical conditions. Variation of conversion with A/V ratio at two different temperatures is shown in figure 6. Doping with either calcium or potassium decreased the activity of  $V_2O_5/ZrO_2$  catalyst but the effect was more pronounced with potassium. At a loading of A/V=0.5, the activity of potassium doped catalyst decreased drastically whereas

calcium doped catalyst still showed considerable activity. The main products for both doped and undoped catalysts were propene, CO and  $CO_2$ . At higher conversion, traces of ethylene were also observed but

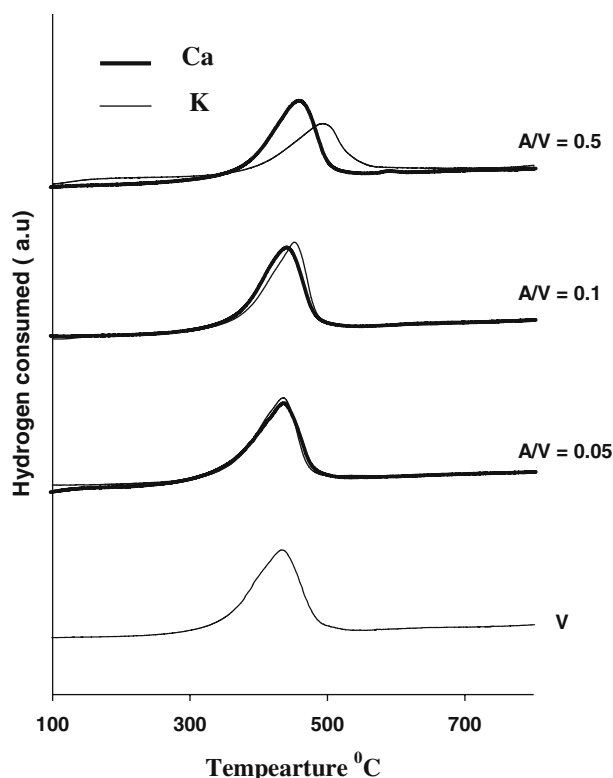


Figure 4. TPR profiles of undoped and doped  $V_2O_5/ZrO_2$  catalyst.

Table 3  
Analysis of TPR profiles for undoped and doped  $V_2O_5/ZrO_2$  catalysts

Catalyst	Extent of reduction	% $H_2$ consumed		Peak Temperature $^{\circ}C$	
		Peak1	Peak2	Peak1	Peak2
5V	0.81	71.4	28.6	414	439
Ca <sub>0.05</sub> V	0.74	70.0	30.0	413	440
Ca <sub>0.1</sub> V	0.75	69.2	30.8	419	441
Ca <sub>0.5</sub> V	0.69	50.8	49.1	430	463
K <sub>0.05</sub> V	0.70	69.0	30.9	418	444
K <sub>0.1</sub> V	0.70	67.8	32.2	427	453
K <sub>0.5</sub> V	0.49	20.5	79.5	435	493

decreased with increase in A/V ratio. The product selectivities at 400  $^{\circ}C$  are plotted as a function of conversion for different A/V atomic ratio in figure 7. Conversion was varied by changing W/ $F_{AO}$  ratio at the same temperature. Due to very low activity of K<sub>0.5</sub>V, selectivity over a wide conversion range could not be obtained for this catalyst. Figure 7a shows that addition of dopants increased the selectivity of propene. For both calcium and potassium, with an increase in A/V ratio the propene selectivity increased and the effect was more significant at higher loading. With an increase in the conversion, the selectivity of propene decreased for all the catalysts caused by increasing secondary reactions to carbon oxides. This is reflected in figure 7(b) and (c), which show that selectivity of both CO and CO<sub>2</sub> increased with increasing conversion. The CO selectivity decreased with increase in loading for both calcium as well as potassium doped catalyst. Selectivity of CO<sub>2</sub> increased with addition of calcium but for potassium, the change depended upon extent of loading (figure 7c). The increase in selectivity of CO<sub>2</sub> with increase in conversion was more for the doped catalysts than that for the undoped catalyst.

Initial selectivities of the products were determined for all the catalysts and are presented in table 5. C<sub>3</sub>H<sub>6</sub>, CO and CO<sub>2</sub>, the main products, were also the primary products for each catalyst. It can be observed that, at low loading ( $\leq A/V = 0.1$ ), addition of dopants increased the initial selectivity of propene with simultaneous decrease in CO selectivity. The CO<sub>2</sub> selectivity was mostly unaffected. At high loading ( $A/V = 0.5$ ), there was a significant increase in CO<sub>2</sub> selectivity and propene selectivity was lowered.

#### 4. Discussion

The characterization results show that addition of both calcium and potassium affects the physicochemical properties of the  $V_2O_5/ZrO_2$  catalyst. The extent and nature of interaction with the surface vanadia species varied with the dopant and its amount. The comparison of EPR spectra of fresh and used catalysts reflects that both the dopants stabilize the vanadium in +5 oxidation state, and the effect was more prominent for calcium doped catalyst. With addition of potassium, the shift of the 1031  $cm^{-1}$  peak in the Raman spectra to lower wave number implies a weakening of the V=O bond [17]. The disappearance of this band on introduction of calcium implies a stronger interaction with the terminal V=O, resulting in the loss of its double bond character. The modification in polyvanadate band also confirms change in the structure of surface vanadates in presence of dopants. Both the EPR and Raman studies predict a stronger interaction between calcium and vanadium compared to potassium. This is in spite of the fact that surface concentration of calcium is lower than that of potassium. Though the exact nature of the interaction between the dopants and the surface vanadia species is not yet well understood, the much stronger

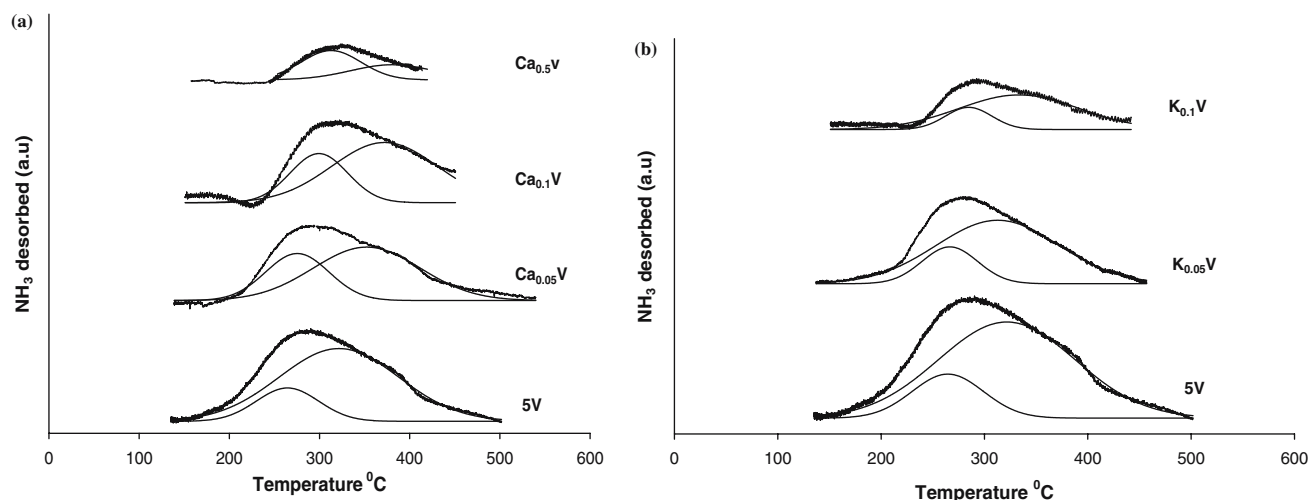


Figure 5.  $NH_3$ -TPD profiles of undoped and doped  $V_2O_5/ZrO_2$  (a) Ca<sub>x</sub>V (b) K<sub>x</sub>V.



Table 4  
Analysis of  $NH_3$ -TPD profiles for undoped and doped  $V_2O_5/ZrO_2$  catalysts

Catalyst	Total $NH_3$ ( $\mu\text{mol } NH_3/\text{g}$ )	% $NH_3$ desorbed		Peak temperature $^{\circ}\text{C}$	
		Peak1	Peak2	Peak1	Peak2
V	104.4	19.2	80.8	265	322
$Ca_{0.05}V$	84.7	34.3	65.7	275	352
$Ca_{0.1}V$	80.7	30.8	69.2	292	374
$Ca_{0.5}V$	29.2	56.8	43.2	313	380
$K_{0.05}V$	62.8	20.8	79.2	266	312
$K_{0.1}V$	33.3	19.7	80.2	284	333
$K_{0.5}V$	a	—	—	—	—

a: very low

interaction with calcium might have been caused by the its higher positive charge.

It is well accepted that the oxidative dehydrogenation reactions on supported vanadia catalyst proceed via the Mars-van Krevelen mechanism consisting of reduction of the oxide catalyst surface by hydrocarbon and subsequent reoxidation by gas phase oxygen [18–20]. The redox property of the catalyst is therefore expected to play an important role in these reactions. Results in literature attribute the higher activity of the supported vanadia catalysts for partial oxidation of methanol, ethane, toluene, o-xylene and oxidative dehydrogenation of propane [21–25] to their lower reduction temperature.

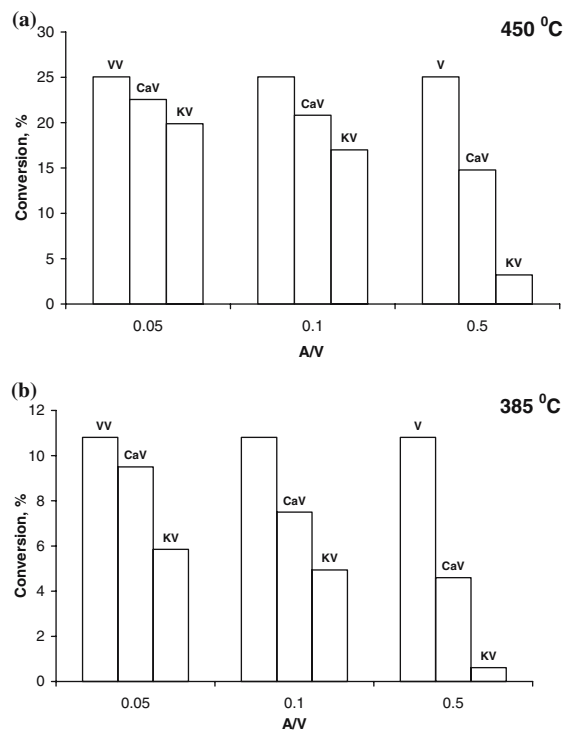


Figure 6. Activity of undoped and doped  $V_2O_5/ZrO_2$  catalyst (a) 450  $^{\circ}\text{C}$  (b) 385  $^{\circ}\text{C}$ .

In this study, presence of two peaks in TPR profiles of the catalysts suggest that at least two types of reducible vanadia species are present on the surface, the relative concentration depending on the nature of dopants and its amount. Roozeboom *et al.* [26] have also reported the presence of two types of surface vanadia species for  $V_2O_5/ZrO_2$  and  $V_2O_5/Al_2O_3$  catalyst. Our earlier study [5] has shown that catalyst with dominantly monovanadates structure as well as a catalyst with more complicated polyvanadate structure show higher reduction temperature than the polyvanadate structure obtained at vanadia surface concentration of  $5VO_x/\text{nm}^2$ . Therefore, it is suggested that the lower temperature peak (table 3) corresponds to reduction of vanadia species with less complicated polyvanadates structure whereas the high temperature peak corresponds to reduction of both monovanadates and complicated polyvanadates species.

Addition of dopants shifts the reduction peaks to higher temperature as well as reduces the extent of reduction of the  $V_2O_5/ZrO_2$  catalyst. For calcium doped catalyst at low loading, the decrease in extent of reduction results in lower activity. At higher loading increase in reduction temperature as well as significant lowering in extent of reduction, both contribute to the substantial lowering of the activity. The increase in  $P_2/P_1$  ratio also seems to contribute in reducing the activity. The very low activity of the  $K_{0.5}V$  catalyst can also be explained on the basis of increase in the reduction temperature, a decrease in extent of reduction as well as a significant increase in  $P_2/P_1$  ratio. At the same A/V ratio, compared to calcium, potassium doped catalyst always showed a higher reduction temperature, lower extent of reduction, higher  $P_2/P_1$  ratio and therefore lower activity.

Since repetitive redox cycles occur during oxidative dehydrogenation of propane, the catalyst that can undergo these redox cycles without any significant modification of structures that affect reducibility is expected to be more stable and active. These reaction conditions can be simulated by alternate cycles of TPR–TPO experiments. It has been found that more stable and active catalysts undergo less change in the TPR profiles during repetitive redox cycles in the TPR–TPO experiments [27]. The higher reduction temperature in second cycles for the doped catalysts implies that for these catalysts the re-reduction is more difficult than for undoped. This may be another reason for the lower activity of the doped catalysts. The significant change in the reduction profiles when the doped catalysts are heated to higher temperature suggest a considerable change in the surface vanadia structure after the first TPR cycle. Therefore it can be concluded that stability of the catalyst is reduced in presence of dopants.

The selectivity to propene varied in the order  $K_xV > Ca_xV > 5V$ . Previous studies have shown that the acid-base property of the catalyst surface influences the

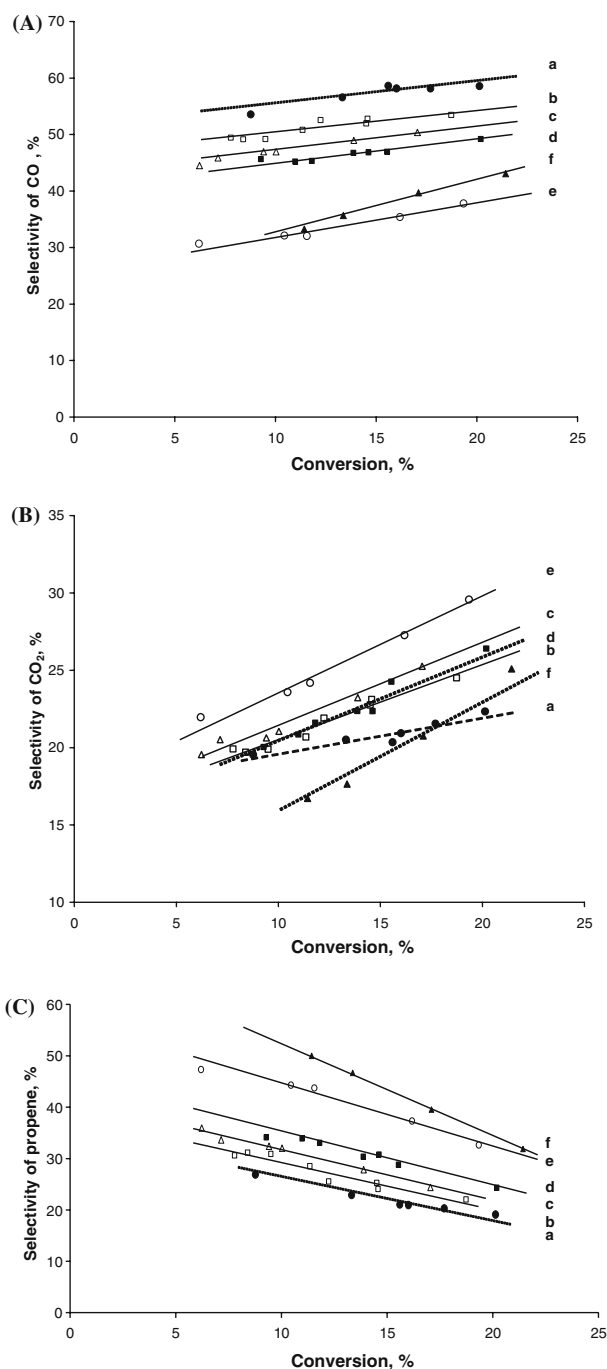


Figure 7. Selectivity of the products at 400°C for undoped and doped  $V_2O_5/ZrO_2$  catalyst. (A) Propene (B) CO (C)  $CO_2$ ; (a) 5V (b)  $Ca_{0.05}V$  (c)  $Ca_{0.1}V$  (d)  $K_{0.05}V$  (e)  $Ca_{0.5}V$  (f)  $K_{0.1}V$ .

surface adsorption-desorption of the reaction intermediates and products, and thereby affects the process selectivity [28]. The lower acidity of the catalyst surface facilitates desorption of propene, the basic intermediate product and prevent its further oxidation to carbon oxides. The higher strength of the acid sites is also expected to hold the alkene more strongly favoring its deep oxidation. Hence, at the same level of acidity, increase in the strength of the sites is expected to lower the selectivity. Lowest selectivity of propene for undoped catalysts can be explained on basis of its highest

acidity. A decrease in the total acidity with addition of dopants facilitated easier desorption of propene from the surface resulting in higher propene selectivity. The higher strength of the acid sites of the doped catalyst at high loading ( $A/V = 0.5$ ) may have caused its higher  $CO_2$  selectivity, since it is well known that stronger acid sites promote total oxidation [29].

According to the catalytic results shown in figure 7 and table 5, the ODH of propane can be represented by



Table 5  
Initial product selectivities for undoped and doped V<sub>2</sub>O<sub>5</sub>/ZrO<sub>2</sub> catalysts

Catalyst	Product selectivity (%)		
	Propene	CO	CO <sub>2</sub>
5V	64.3	23.3	12.6
Ca <sub>0.05</sub> V	66.6	21.6	11.8
Ca <sub>0.1</sub> V	69.6	19.5	10.9
Ca <sub>0.5</sub> V	66.4	14.9	18.85
K <sub>0.05</sub> V	68.8	19.7	10.9
K <sub>0.1</sub> V	73.9	16.1	10.2
K <sub>0.5</sub> V	60.3	11.3	28.4

Scheme 8 in which propene is a primary product which can be further oxidized. CO and CO<sub>2</sub> are produced both by the primary combustion of propane and by secondary decomposition of propene.

The doping resulted in modification of the relative reaction rates. For undoped V<sub>2</sub>O<sub>5</sub>/ZrO<sub>2</sub> catalyst, initial selectivity of CO is higher compared to CO<sub>2</sub> (Fig 7). At high loading of dopants (A/V=0.5),  $k_3/k_2$  increased significantly i.e.  $(k_3/k_2)_{\text{doped}} > (k_3/k_2)_{\text{undoped}}$ . Further, with increasing conversion, significant increase in CO<sub>2</sub> selectivity for modified catalysts implies an increase in  $k_5/k_4$  and/or  $k_6/k_4$  ratio.

The reduced centers V<sup>+4</sup> are believed to be the reactive intermediates involved in the Mars-van Krevelen redox cycles [30]. Both V<sup>+5</sup> and V<sup>+4</sup> were reported to catalyze the oxidative dehydrogenation of propane but V<sup>+4</sup> was observed to be more selective though less active than V<sup>+5</sup> [13]. The role of V<sup>+4</sup> centers in V<sub>2</sub>O<sub>5</sub>/ZrO<sub>2</sub> catalysts is not too clear. The undoped catalyst which has highest V<sup>+4</sup> / V<sup>+5</sup> ratio, shows highest activity but lowest selectivity of propene. With addition of dopants the ratio decreased whereas the selectivity increased. However, when the doped catalysts are compared among themselves, the calcium doped catalyst with lower V<sup>+4</sup> / V<sup>+5</sup> ratio was found to be less selective than the potassium doped catalyst with higher concen-

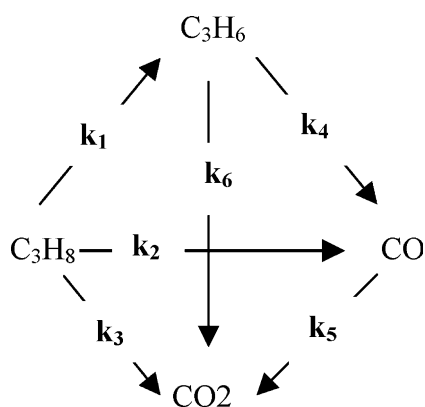
tration of reduced centers. Therefore no definite conclusion can be drawn and further detailed study is needed to explain this anomaly.

## 5. Conclusion

Addition of calcium and potassium affects the physicochemical properties of the V<sub>2</sub>O<sub>5</sub>/ZrO<sub>2</sub> catalyst. The extent and nature of interaction varied with the dopant and its amount. Calcium and potassium essentially stabilize the V (V) oxidation state and interact with the V=O bond in V<sub>2</sub>O<sub>5</sub>/ZrO<sub>2</sub> catalyst. Although, no major redistribution of surface vanadia species was observed on addition of dopants, the vanadia structure was definitely affected. Interaction between calcium and vanadium was more intense though surface concentration of calcium was less than that of potassium. Higher positive charge on calcium may be one of the reasons for this. For doped catalysts, higher reduction temperature, lower extent of reduction and increasing resistance to undergo redox cycles, caused by structural change of the surface vanadates in presences of dopants, lowered the activity. On the other hand, addition of dopants reduced the acidic sites on the catalyst surface, facilitating desorption of propene and increasing its selectivity. Potassium was more effective in increasing the propene selectivity. The dopants also caused a change in the relative reaction rates on the V<sub>2</sub>O<sub>5</sub>/ZrO<sub>2</sub> catalyst.

## References

- [1] S. Albrecht, G. Wendt, G. Lippold, A. Adamski and K. Dyrek, Solid State Ionics 101–103 (1997) 909.
- [2] Y. Toda, T. Ohno, F. Hatayama and H. Miyata, Appl. Catal. A 207 (2001) 273.
- [3] Z. Feng, W.S. Postula, C. Erkey, C.V. Philip, A. Akgerman and R.G. Anthony, J. Catal. 148 (1994) 84.
- [4] T. Ohno, Y. Bunno, F. Hatayama, Y. Toda and H. Miyata, Appl. Catal. B 30 (2001) 421.
- [5] M. De and D. Kunzru, Catal. Lett. 96 (2004) 33.
- [6] H. Toraya, M. Yoshimura and S. Somiya, J. Am. Ceram. Soc. 67 (1984) C119.
- [7] G.K. Chuah and S. Jaenicke, Appl. Catal. A 163 (1997) 261.
- [8] E.E. Platero and M.P. Mentruit, Langmuir 13 (1997) 3150.
- [9] A. Khodakov, J. Yang, S. Su, E. Iglesia and A.T. Bell, J. Catal. 177 (1998) 343.
- [10] G.T. Went, S.T. Oyama and A.T. Bell, J. Phys. Chem. 94 (1990) 4240.
- [11] X. Gao, J. Jehng and I.E. Wachs, J. Catal. 209 (2002) 43.
- [12] T. Blasco, A. Galli, J.M. Lopez Nieto and F. Trifiro, J. Catal. 169 (1997) 203.
- [13] P. Rybarczyk, H. Berndt, J. Radnik, M.M. Pohl, O. Buyevskaya, M. Baerns and A. Brückner, J. Catal. 202 (2001) 45.
- [14] M. Panizza, C. Resini, F. Raccoli, G. Busca, R. Catani and S. Rossini, Chem. Eng. J. 93 (2003) 181.
- [15] W. Chu, T. Echizen, Y. Kamiya and T. Okuhara, Appl. Cat. A 259 (2004) 199.
- [16] J. Rätty and T.A. Pakkanen, Appl. Cat. A 208 (2001) 169.
- [17] G. Garcia Cortez, J.L.G. Fierro and M.A. Bañares, Catal. Today 78 (2003) 219.



Scheme 1. Reaction network for the oxidative dehydrogenation of propane.

- [18] E.A. Mamedov and V. Cortés Corberán, *Appl. Catal. A* 127 (1995) 1.
- [19] D. Creaser, B. Andersson, R.R. Hudgins and P.L. Silveston, *Appl. Catal. A* 187 (1999) 147.
- [20] K. Chen, A. Khodakov, J. Yang, A.T. Bell and E. Iglesia, *J. Catal.* 186 (1999) 325.
- [21] G. Deo and I.E. Wachs, *J. Catal.* 146 (1994) 323.
- [22] M.A. Bañares, M.V. Martínez-Huerta, X. Gao, J.L.G. Fierro and I.E. Wachs, *Catal. Today* 61 (2000) 295.
- [23] J. Van Hengstum, J.G. Van Ommen, H. Bosh and P.J. Gellings, *Appl. Catal. A* 8 (1983) 369.
- [24] S. Anniballi, F. Cavani, A. Guerrini, B. Panzacchi, F. Trifirò, C. Fumagalli, R. Leanza and G. Mazzoni, *Catal. Today* 78 (2003) 117.
- [25] A. Lemonidou, L. Nalbandian and I.A. Vasalos, *Catal. Today* 61 (2000) 333.
- [26] F. Roozeboom, M.C. Mittelmeijer-Hazeleger, J.A. Moulijn, J. Medema, V.H.J. de Beer and P.J. Gellings, *J. Phys. Chem.* 84 (1980) 2783.
- [27] S. Varma, B.N. Wani and N.M. Gupta, *Appl. Catal. A* 205 (2001) 295.
- [28] T. Blasco and J.M. Lopez Nieto, *Appl. Catal. A* 157 (1997) 117.
- [29] H.W. Zanthoff, M. Lahmer, M. Baerns, E. Klemm, M. Seitz and G. Emig, *J. Catal.* 172 (1997) 203.
- [30] M.D. Argyle, K. Chen, C. Resini, C. Krebs, A.T. Bell and E. Iglesia, *J. Phys. Chem. B* 108 (2004) 2345.